

144. Magnetic-Field-Dependent Electronic Relaxation of Gd^{3+} in Aqueous Solutions of the Complexes $[Gd(H_2O)_8]^{3+}$, $[Gd(\text{propane-1,3-diamine-}N,N,N',N'\text{-tetraacetate})(H_2O)_2]^-$, and $[Gd(N,N'\text{-bis}(N\text{-methylcarbamoyl)methyl})\text{-3-azapentane-1,5-diamine-3},N,N'\text{-triacetate})(H_2O)]$ of Interest in Magnetic-Resonance Imaging

by **D. Hugh Powell** and **André E. Merbach***

Institute of Inorganic and Analytical Chemistry, University of Lausanne, Place du Château 3,
CH-1005 Lausanne

and **Gabriel González**

Department of Inorganic Chemistry, University of Barcelona, Avenue Diagonal 647,
E-08028 Barcelona

and **Ernö Brücher** and **Károly Micskei**

Institute of Inorganic and Analytical Chemistry, Kossuth University, H-4010 Debrecen

and **M. Francesca Ottaviani**

Department of Chemistry, University of Florence, I-50121 Florence

and **Klaus Köhler** and **Alex von Zelewsky**

Institute of Inorganic Chemistry, University of Fribourg, Perolles, CH-1700 Fribourg

and **Oleg Ya. Grinberg** and **Yakob S. Lebedev**

Institute of Chemical Physics, Russian Academy of Sciences, 117977 Moscow V-334, Kosygina 4, Russia

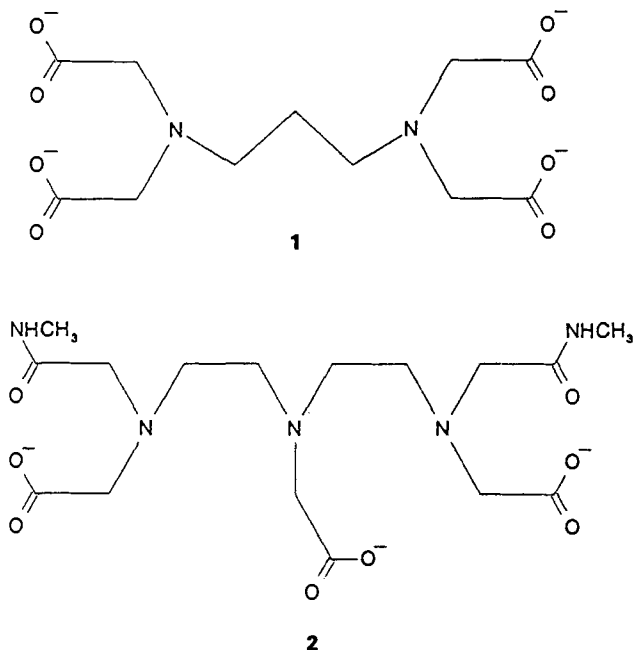
(28. IV. 93)

EPR Spectra have been measured for aqueous solutions of a series of Gd^{3+} complexes at variable temperature and a range of magnetic fields; S-band (0.14 T), X-band (0.34 T), Q-band (1.2 T), and 2-mm-band (5.0 T). The major contribution to the observed line widths is magnetic-field-dependent and is interpreted as being due to the modulation of the zero-field splitting produced by distortion of the complexes from perfect symmetry. The transverse and longitudinal relaxation matrices for an 8S ion with such an interaction have been calculated using *Redfield* theory with vector-coupling methods, and diagonalised numerically to obtain relaxation rates and intensities for the degenerate transitions which contribute to the multiplet. The observed line width, which is inversely proportional to the magnetic field at low temperatures, is best described by the intensity-weighted mean transverse relaxation time for the four transitions with non-zero intensity. A least-squares fit of the data yields the square of the zero-field splitting tensor, Δ^2 , and a correlation time, τ_c , with activation energy, E_v . The physical significance of these parameters and the extent of validity of the theoretical approach are considered. The parameters are used to predict the magnetic-field dependence of the longitudinal and transverse electronic relaxation times, which are discussed in the context of their relevance to 1H -NMR relaxivity.

Introduction. – Complexes of the Gd^{3+} ion in aqueous solution are generating much interest as actual and potential contrast agents in biomedical magnetic resonance imaging (MRI) [1]. To produce contrast, the complex must modify significantly the proton relaxation rates of water in its vicinity. Around a paramagnetic ion, the bulk water proton relaxation rates are enhanced either due to long-range interactions ('outer-sphere' relax-

ation) or to short-range interactions mediated by exchange with coordinated molecules ('inner-sphere' relaxation). Where there is one or more H₂O molecule coordinated in the complex, the relaxation enhancement, or relaxivity, is dominated by the 'inner-sphere' effect [1] [2]. This effect is determined by four correlation times; the time for rotation of the complex, τ_c , the residence time of a H₂O proton in the first coordination sphere, τ_m , and the longitudinal and transverse electronic relaxation times, T_{1e} and T_{2e} , respectively [1]. The 'outer-sphere' relaxivity is determined by the translational motion of outer-sphere H₂O molecules, and by T_{1e} and T_{2e} [1]. The contribution of this effect to the total proton relaxivity may be estimated to be 10–50%, depending on the number of inner-sphere H₂O molecules [3]. A knowledge of the electronic relaxation times of Gd³⁺ complexes in solution and an understanding of the factors that determine these times are, therefore, important in the search for new MRI contrast agents. It has been observed [3] that, for certain Gd³⁺ complexes, there is a discrepancy between T_{2e} obtained from X-band (0.34 T) EPR line widths and the electronic relaxation time at zero field, τ_{s0} , determined by fitting the field dependence of the proton relaxivity obtained from NMR-dispersion (NMRD) measurements. It is, therefore, important to investigate the magnetic-field dependence of the electronic relaxation times.

Southwood-Jones *et al.* [4] measured the temperature dependence of the ¹⁷O-NMR relaxation rates of the complexes [Gd(H₂O)₈]³⁺ and [Gd(**1**)(H₂O)₂]⁻ (**1** = propane-1,3-diamine-*N,N,N',N'*-tetraacetate) in order to determine the rate and mechanism of exchange of bound H₂O with the bulk. The relaxation rates are determined by a correlation time $\tau^{-1} = k_{ex} + T_{1e}^{-1}$, so that a knowledge of T_{1e} is required in order to extract the water exchange rate, k_{ex} . The above-mentioned authors measured the EPR line widths of



solutions of $[\text{Gd}(\text{H}_2\text{O})_8]^{3+}$ at X-band and Q-band and of $[\text{Gd}(\mathbf{1})(\text{H}_2\text{O})_2]^{2-}$ at X-band. They related the line widths to T_{2e} and, using the theory of *McLachlan* [5], extrapolated values of T_{1e} at the NMR magnetic fields. Workers at the Lausanne laboratory have extended ^{17}O -NMR measurements to a number of Gd^{3+} complexes of interest as MRI contrast agents [2] [6]. Multiple-field measurements for $[\text{Gd}(\mathbf{1})(\text{H}_2\text{O})_2]^-$ and $[\text{Gd}(\mathbf{2})(\text{H}_2\text{O})]$ ($\mathbf{2} = N, N'$ -bis[(*N*-methylcarbamoyl)methyl]-3-azapentane-1,5-diamine-3, *N, N'*-triacetate) suggest that the field dependence of the electronic relaxation is not as expected from *McLachlan*'s equations [5]. For the correct interpretation of these results, therefore, we would like to know the electronic relaxation rates of these complexes in solution over as wide a range of magnetic field as possible, particularly at high fields (for the NMR measurements the field was in the range 1.4 T to 9.4 T).

We present here the results of variable-temperature EPR line width measurements of solutions of the complexes¹⁾ $[\text{Gd}(\text{H}_2\text{O})_8]^{3+}$, $[\text{Gd}(\mathbf{1})(\text{H}_2\text{O})_2]^-$, and $[\text{Gd}(\mathbf{2})(\text{H}_2\text{O})]$ at a number of frequencies from S-band (corresponding to 0.14 T) to 2-mm-band (corresponding to 5.0 T). We interpret the results using the idea of a transient zero-field splitting (ZFS) induced by distortion of the complexes. Such an interaction has been proposed to explain the larger than expected EPR line widths of a number of metal ions with spin $S > 1/2$ [10–13], and has been successfully applied to a series of Gd^{3+} complexes [4] [14]. We will show, however, that some modification of the approach used to relate theory to experimental line widths will be necessary to explain the line width at high magnetic field, particularly for the polyaminocarboxylate chelates of interest in MRI that are presented here.

Relaxation Theory. – It has been proposed that the EPR line widths of metal ions with spin $S > 1/2$ in solution are determined by a transient ZFS, induced by distortions of the complexes [10–13]. This mechanism was suggested initially, since the observed line widths were much larger than expected from estimates of the contributions from other relaxation mechanisms, *e.g.*, modulation of the anisotropic *g*-factor and spin rotation. The interaction may be modulated either by rotation of the complex or by the change of the axis of distortion, but the form of the equations describing the interaction is identical in the two cases [13].

Gd^{3+} is an ^8S ion, with no nuclear hyperfine structure [15]. The observed line shape will, therefore, be a combination of seven degenerate electronic transitions. If the line shape is *Lorentzian*, the peak-to-peak line width, ΔH_{pp} , of the derivative spectrum is related to an overall transverse relaxation rate, $1/T_{2e}$, by [14]

$$\frac{1}{T_{2e}} = (g\mu_B\pi\sqrt{3}/h)\Delta H_{\text{pp}} \quad (1)$$

where *g* is the *Landé g*-factor and the other terms have their usual meanings. Analytical expressions for the transverse and longitudinal electronic relaxation rates were derived by

¹⁾ The structures implied for the complexes are based for the aqua complex on neutron-diffraction data for lanthanide-ion solutions [7], for the complex with **1** on kinetic and thermodynamic measurements [8] and on the magnitude of the ^{17}O -NMR chemical shift [2] and for the complex with **2** on the crystal structure of the *Dy* (**2**) analogue [9] and the ^{17}O -NMR chemical shift [6]. UV/VIS Spectra for all three complexes show only one species present in solution in the temperature range 20° to 95° [2] [6].

McLachlan [5], using an operator approach to the *Redfield* theory [16] and the concept of the mean relaxation rates

$$\langle 1/T_{1e} \rangle = \sum_i \frac{I_i}{T_{1ei}} \quad (2)$$

$$\langle 1/T_{2e} \rangle = \sum_i \frac{I_i}{T_{2ei}} \quad (3)$$

where I_i , T_{1ei} , and T_{2ei} are the intensity and longitudinal and transverse relaxation times for each electronic transition. He obtained the expressions

$$\langle 1/T_{1e} \rangle = \frac{1}{25} \Delta^2 \tau_v \{4S(S+1) - 3\} [J_1 + 4J_2] \quad (4)$$

$$\langle 1/T_{2e} \rangle = \frac{1}{50} \Delta^2 \tau_v \{4S(S+1) - 3\} [3J_0 + 5J_1 + 2J_2] \quad (5)$$

where, in this case, Δ^2 is the trace of the square of the ZFS tensor, S is the electron spin and

$$J_n = \frac{1}{1 + (n\omega\tau_v)^2} \quad (6)$$

where ω is the resonance frequency and τ_v is the correlation time for the modulation of the ZFS. The mean line width associated with the mean transverse relaxation rate (5) is shown as a function of $\omega\tau_v$ in *Fig. 1a*. Assuming that τ_v depends exponentially on temperature

$$\tau_v = \tau_v^{298} \exp\{E_v/R(1/T - 1/298.15)\} \quad (7)$$

where τ_v^{298} is the value of τ_v at 298.15 K and E_v is the activation energy for the modulation, one can calculate the expected temperature and field dependence of the line width (*Fig. 1b*). The line width increases monotonically as the temperature is reduced, with a point of inflection when $\omega\tau_v \approx 1$. This is the theory applied by *Southwood-Jones et al.* to Gd^{3+} solutions [4]. As pointed out by *McLachlan*, the equations are only valid in the regime $\omega\tau_v \ll 1$.

Hudson and *Lewis* used *Redfield* theory with vector-coupling methods to obtain the transverse relaxation matrix for an 8S ion [15]. The matrix elements are given by²⁾

$$R_{\alpha\beta\beta'} = (2L+1)^{-1} |\langle S \| T^{(2)} \| S \rangle|^2 \{ 2C(SLS; \alpha, \beta - \alpha) C(SLS; \alpha', \beta' - \alpha') j(\alpha - \beta) - \delta_{\alpha\beta} \sum_{\gamma} C^2(SLS; \gamma, \beta' - \gamma) j(\beta' - \gamma) - \delta_{\alpha\beta'} \sum_{\gamma} C^2(SLS; \gamma, \beta - \gamma) j(\beta - \gamma) \} \sum_q F^{(L,q)} F'^{(L,q)*} \quad (8)$$

²⁾ The equation given here differs slightly from that given by *Hudson* and *Lewis* [15] in that the $\beta' - \gamma$ and $\beta - \gamma$ terms in the vector-coupling coefficients are reversed. We have checked that the equation given here gives results in agreement with those of *Hudson* and *Lewis* for the T_2 matrix for 8S , and with the T_1 and T_2 matrices for 6S calculated using operator techniques [17].

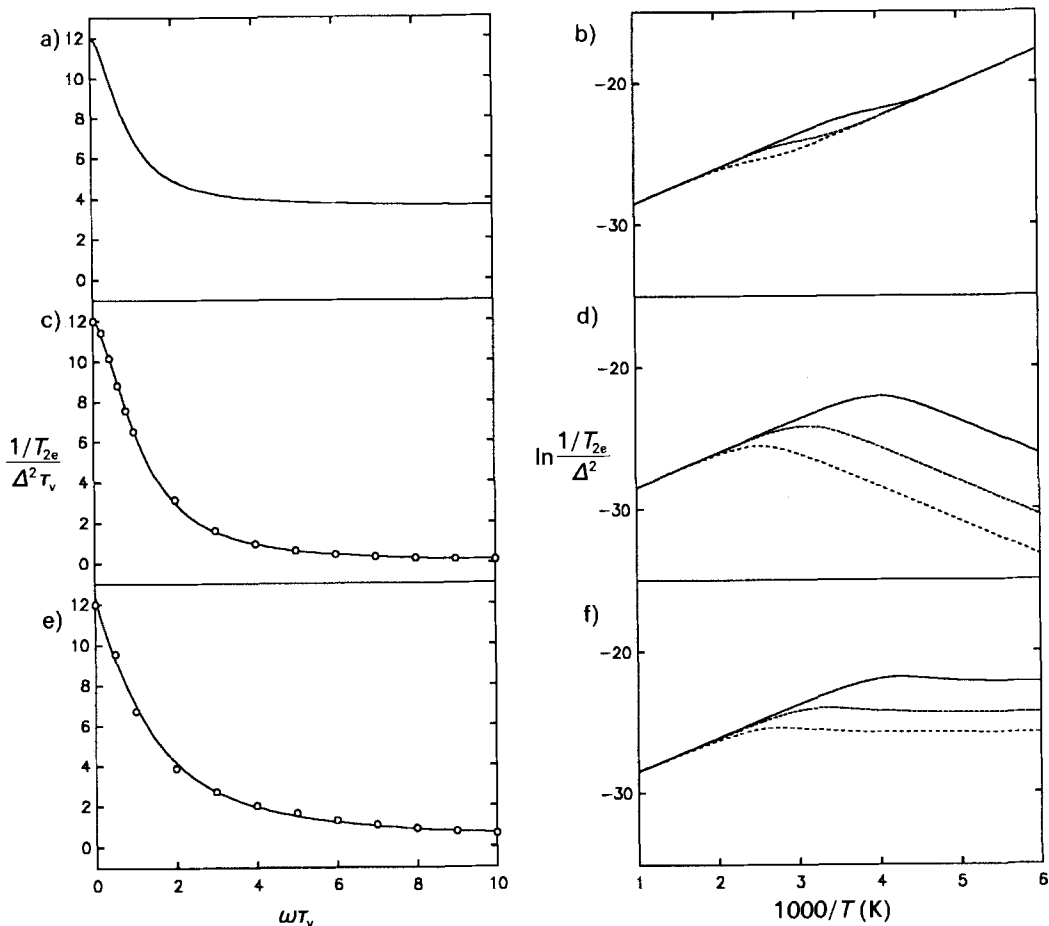


Fig. 1. Calculated reduced line widths as a function of $\omega\tau_v$, a) using McLachlan's theory, or using the Redfield relaxation matrix of Hudson and Lewis, assuming the overall line width is determined by c) the narrowest transition or e) the mean relaxation time (see text for details). The corresponding temperature dependencies were calculated using $\tau_v^{298} = 1.0 \times 10^{-11}$ s and $E_v = 20$ kJ mol $^{-1}$ in Eqn. 7 at 0.14 T (dashed line), 1.2 T (heavy dashed line), and 5.0 T (solid line), and are shown in (b), (d), and (f), respectively.

where $\alpha, \alpha', \beta, \beta'$ and γ refer to the spin states $m_s = 7/2, 5/2 \dots -7/2$, C are the Clebsch-Gordan or vector-coupling coefficients [18]³, $T^{(2)}$ is a time independent operator in a space-fixed axis system, $F^{(2)}$ is a time dependent tensor operating on spatial variables and $j(\alpha - \beta) = \tau_v J_n$ where $n = |\alpha - \beta|$. The reduced matrix element is given by $\langle 7/2 || T^{(2)} || 7/2 \rangle = \langle 7/2 || 7/2 S_+^2 || 7/2 \rangle / C(7/2, 2, 7/2; 7/2, -2) = \sqrt{315/2}$ and $\sum_q F^{(L,q)} F'^{(L,q)*} = \Delta^2$. Using

³) The notation used here and in [15] for the vector-coupling coefficients is related to that of [18] by $C(SLS; m_1 m_2) = (j_1 L m_1 m_2 | j_1 L j m)$ with $j = j_1 = S$ and $m = m_1 + m_2$.

the fact that $\Delta m_s = \pm 1$, the transverse relaxation matrix is constructed from the terms $\alpha - \alpha' = 1, \beta - \beta' = 1$, for $\alpha = 7/2, 5/2 \dots - 5/2$, and $\beta = 7/2, 5/2 \dots - 5/2$, giving

$$\mathbf{R}_2 = \Delta^2 \tau_v \mathbf{M}_2 \quad (9)$$

where

$$\mathbf{M}_2 = \begin{pmatrix} A & E & F & 0 & 0 & 0 & 0 \\ E & B & G & H & 0 & 0 & 0 \\ F & G & C & 0 & I & 0 & 0 \\ 0 & H & 0 & D & 0 & H & 0 \\ 0 & 0 & I & 0 & C & G & F \\ 0 & 0 & 0 & H & G & B & E \\ 0 & 0 & 0 & 0 & F & E & A \end{pmatrix} \quad (10)$$

and

$$A = -(3/5)\{18J_0 + 58J_1 + 22J_2\}$$

$$B = -(3/5)\{8J_0 + 58J_1 + 42J_2\}$$

$$C = -(3/5)\{2J_0 + 26J_1 + 62J_2\}$$

$$D = -(3/5)\{10J_1 + 70J_2\}$$

$$E = (24/5)\sqrt{21}J_1$$

$$F = 6\sqrt{21/5}J_2$$

$$G = (24/\sqrt{5})J_1$$

$$H = 12\sqrt{3}J_2$$

$$I = 24J_2$$

Hudson and *Lewis* did not calculate the corresponding matrix for longitudinal relaxation. This calculation is performed by taking the matrix elements $\alpha = \alpha', \beta = \beta'$, for $\alpha = 7/2, 5/2 \dots - 7/2$ and $\beta = 7/2, 5/2 \dots - 7/2$, giving

$$\mathbf{R}_1 = \Delta^2 \tau_v \mathbf{M}_1 \quad (11)$$

where

$$\mathbf{M}_1 = \begin{pmatrix} A & E & F & 0 & 0 & 0 & 0 & 0 \\ E & B & G & H & 0 & 0 & 0 & 0 \\ F & G & C & I & J & 0 & 0 & 0 \\ 0 & H & I & D & 0 & J & 0 & 0 \\ 0 & 0 & J & 0 & D & I & H & 0 \\ 0 & 0 & 0 & J & I & C & G & F \\ 0 & 0 & 0 & 0 & H & G & B & E \\ 0 & 0 & 0 & 0 & 0 & F & E & A \end{pmatrix} \quad (12)$$

and

$$A = -(3/5)\{42J_1 + 14J_2\}$$

$$B = -(3/5)\{74J_1 + 30J_2\}$$

$$C = -(3/5)\{42J_1 + 54J_2\}$$

$$D = -\{6J_1 + 42J_2\}$$

$$E = (126/5)J_1$$

$$F = 42/5J_2$$

$$G = 96/5J_1$$

$$H = 18J_2$$

$$I = 6J_1$$

$$J = 24J_2$$

Numerical diagonalisation of the relaxation matrices (Eqns. 10 and 12) yields eigenvalues λ_i and eigenvectors ξ_i as a function of $\omega\tau_v$. These are related to the relaxation rate and relative intensity of each electronic transition by

$$\frac{1}{T_{1ei}}, \frac{1}{T_{2ei}} = -A^2\tau_v\lambda_i \quad (13)$$

$$I_i = (\xi_i \cdot \mathbf{X})^2 / \sum_j (\xi_j \cdot \mathbf{X})^2 \quad (14)$$

where \mathbf{X} is the vector composed of the elements $X_{\alpha\alpha'} = \langle \alpha | S_x | \alpha' \rangle = h\sqrt{(I/2 - \alpha + 1)(I/2 + \alpha)}$ for transverse relaxation or $X_z = \langle \alpha | S_z | \alpha \rangle = h\alpha$ for longitudinal relaxation [16].

For transverse relaxation there are four transitions with non-zero intensity. The relaxation rates and intensities for the individual transitions are shown as a function of $\omega\tau_v$ in Fig. 2. The overall derivative line shape, $I'(\omega)$, will be a superposition of these four transitions [16]

$$I(\omega) = \text{Re} \int_{-\infty}^{\infty} G^+(t) \exp(i\omega t) dt \quad (15)$$

$$G^+(t) = \exp(-i\omega t) \sum_i I_i \exp(-t/T_{2ei})$$

To interpret our experimental results, it will be necessary to relate the relaxation rates and intensities for each transition to the overall line width obtained from the approximately *Lorentzian* line shape.

For longitudinal relaxation there are again four transitions and the individual relaxation rates and intensities are shown in Fig. 3. In agreement with calculations for the ^6S system [13], only one transition has significant intensity, so that single exponential relaxation can be expected. The relaxation rate of this transition as a function of $\omega\tau_v$ is well described by the analytical expression of *McLachlan* (Eqn. 4).

We will assume that the observed line shape is *Lorentzian*, which is equivalent to assuming that the spin time correlation function $G^+(t)$ in Eqn. 15 is exponential. *Reuben* [14] treated his EPR line width data for three Gd^{3+} complexes in solution by assuming that the observed spectrum is *Lorentzian*, with transverse relaxation rate equal to that of the

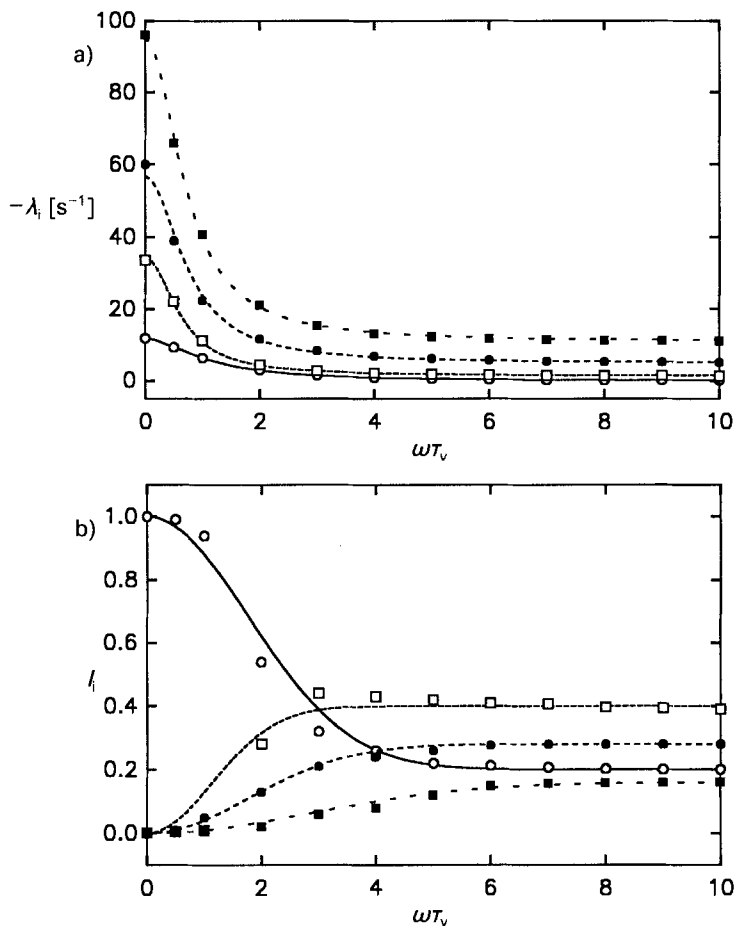


Fig. 2. a) Eigenvalues and b) intensities for the four non-zero electronic transitions calculated by numerical diagonalisation of the Redfield transverse relaxation matrix of Hudson and Lewis [15]. The points represent the results of the calculations, and the curves are drawn as a guide to the eye.

narrowest transition (open circles in Fig. 2). One can fit the relaxation rate for this transition by the empirical expression (Fig. 1c)

$$\frac{1}{T_{2c}} = \Delta^2 \tau_v \left[\frac{(10.5 \pm 0.5)}{1.0 + (0.637 \pm 0.006)(\omega\tau_v)^2} + \frac{(1.5 \pm 0.5)}{1.0 + (9.2 \pm 3.1)(\omega\tau_v)^2} \right] \quad (16)$$

The expected temperature and field dependence of the line width, assuming exponential temperature behaviour for τ_v , is shown in Fig. 1d. The curves show a maximum at $\omega\tau_v \approx 1$. At low temperature and high magnetic field, B , the line width is dependent on the magnetic field.

An approach used by Rubinstein *et al.* [13] in comparing electronic relaxation theory with proton magnetic resonance data for Fe^{3+} , Mn^{2+} ($S = 5/2$), and Cr^{3+} ($S = 3/2$) solu-

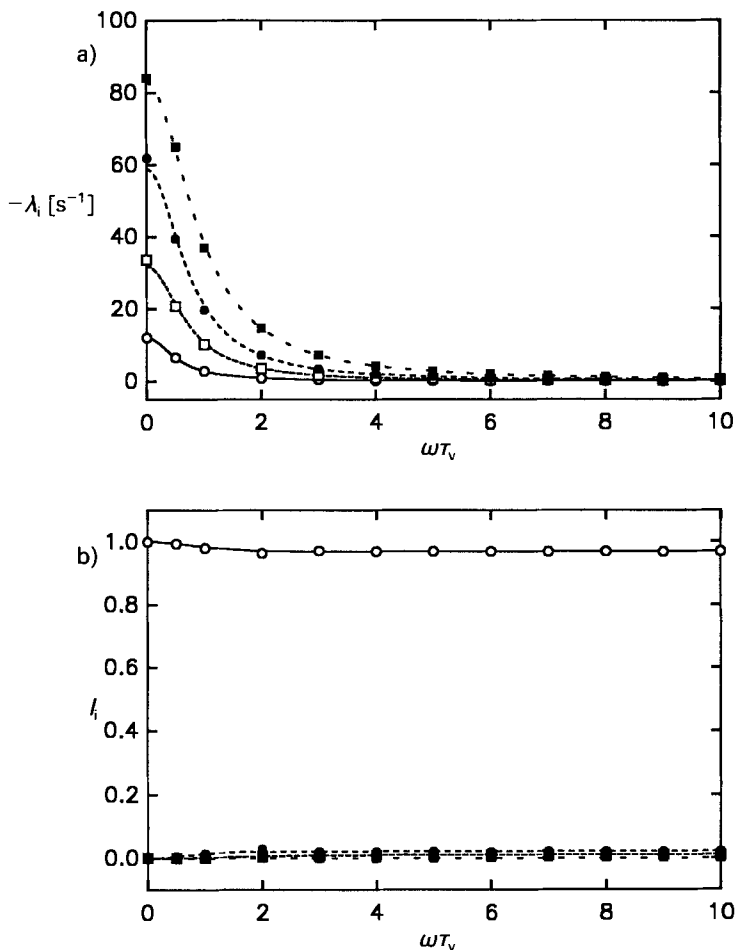


Fig. 3. a) Eigenvalues and b) intensities for the four non-zero electronic transitions calculated by numerical diagonalisation of the Redfield longitudinal relaxation matrix. The points represent the results of the calculations, and the curves are drawn as a guide to the eye.

tions is to assume that the overall line shape is a *Lorentzian*, with width determined by the mean relaxation rate as defined by *McLachlan* (Eqn. 2). This can be calculated from the individual intensities and relaxation rates in Fig. 2. The result is essentially identical to the analytical expression of *McLachlan* (Eqn. 5).

The original reason that *McLachlan* defined this mean relaxation rate was that it is possible to obtain analytical expressions for this quantity. As he pointed out [5], one can equally calculate the mean relaxation times

$$\langle T_{1e} \rangle = \sum_i I_i T_{1ei} \quad (17)$$

$$\langle T_{2e} \rangle = \sum_i I_i T_{2ei} \quad (18)$$

The quantity $\langle T_{2e} \rangle$ represents the mean time between transitions for an electron in a random initial state, and so it may be more physical to associate this, rather than the mean relaxation rate, $\langle 1/T_{2e} \rangle$, with an approximately exponential decay of $G^+(t)$. One can calculate $\langle T_{2e} \rangle$ from the individual intensities and the inverse of the individual line shapes (Fig. 2) and hence calculate an overall relaxation rate. Within the regime $\omega\tau_v \leq 10$, the overall relaxation rate can be parametrised by (Fig. 1e)

$$\frac{1}{\langle T_{2e} \rangle} = \Delta^2 \tau_v \left[\frac{(5.26 \pm 0.53)}{1.0 + (0.372 \pm 0.065)(\omega\tau_v)^2} + \frac{(7.18 \pm 0.85)}{1.0 + (1.24 \pm 0.18)\omega\tau_v} \right] \quad (19)$$

It should be understood that this equation is simply an empirical function fitted to the results of the calculations; the second term should not be interpreted as a special kind of spectral density function. The expected temperature and field dependence derived from this relaxation rate assuming an exponential τ_v is shown in Fig. 1f. As observed for the curve calculated assuming that only the narrowest transition contributes to the line width (Fig. 1d), there is a maximum for $\omega\tau_v \approx 1$, and the line width is dependent on the magnetic field at low temperature and high fields.

Finally, it should be noted that all these approaches are valid only within the *Redfield* limit $\tau_v < T_{1e}, T_{2e}$. *Friedman et al.* [19] have presented a theory for electronic relaxation by modulation of the ZFS which goes beyond this limit into the 'slow-motion' regime. They applied this theory to relaxation in solutions of Ni^{2+} , but their method demands considerable computation, and the variation of the relaxation rates with field does not differ greatly from that calculated with *Redfield* theory.

Experimental. – $\text{Gd}(\text{ClO}_4)_3$ solns. were prepared by dissolving excess Gd_2O_3 in HClO_4 , followed by filtration and pH adjustment with NaOH or HClO_4 solns. The $[\text{Gd}(\text{1})(\text{H}_2\text{O})_2]^-$ complex was prepared using $\text{H}_4\text{-1}$ supplied by Prof. Geier (ETH-Zürich, Switzerland). The necessary quantity of ligand was weighed into double distilled water, and a stoichiometric quantity of $1.0 \text{ mol} \cdot \text{dm}^{-3}$ NaOH for complete deprotonation was added. A stoichiometric quantity of $\text{Gd}(\text{ClO}_4)_3$ was weighed into the ligand soln. and left a day to react. The pH was then regulated using NaOH or HClO_4 solns. The $[\text{Gd}(\text{2})(\text{H}_2\text{O})]$ complex was supplied by *Nycomed Salutar Inc.* (Sunnyvale, U.S.A.). It was dissolved in double distilled water, and the pH was adjusted with HClO_4 soln. The solns. prepared were $\text{Gd}(\text{ClO}_4)_2$ (0.1m, pH 2.0; 0.075m, pH 2.0; 0.05m, pH 2.0; 0.02m, pH 2.0), $[\text{Gd}(\text{1})(\text{H}_2\text{O})_2]^-$ (0.1m, pH 5.0; 0.05m, pH 5.0) and $[\text{Gd}(\text{2})(\text{H}_2\text{O})]$ (0.35m, pH 4.0; 0.11m, pH 3.9; 0.05m, pH 3.9; 0.02m, pH 3.9).

The EPR spectra were measured at S-band (Florence), X-band (Lausanne), Q-band (Fribourg), and 2-mm-band (Moscow). All spectrometers were operated in continuous wave mode. The 2-mm-band spectrometer in Moscow was home-built [20], the S-band and X-band spectrometers were manufactured by *Bruker* and the Q-band spectrometer by *Varian*. For S-, X-, and Q-bands the samples were contained in 5-mm and 1-mm i.d. quartz tubes and 0.3-mm i.d. quartz capillaries, respectively. For the 2-mm-band measurements, the samples were contained between two quartz plates [20]. In all cases, the observed derivative spectrum was a single resonance approximating to a *Lorentzian* line shape. The acquisition parameters, in particular modulation amplitude and microwave power, were varied, and final spectra were recorded with values that did not affect the line width. The peak-to-peak line width was measured from the recorded spectrum either with a ruler or using instrument software. The central frequency of the resonance was, within error, equal to the value expected for a *Landé* g-factor $g = 2.0$. The cavity temp. was varied using electronic temp. control of gas flowing through the cavity. For the S-, X-, and Q-band measurements, the temp. was verified by substituting a thermometer for the sample. Measurements were made at temp. from 0° to the maximum obtainable for each instrument.

Results. – At X-band, no concentration dependence of the line widths was observed, so for S-, X-, and Q-band measurements, relatively concentrated solutions were used in

order to obtain good signal to noise ratios. At 2-mm-band, a significant dependence of the line widths on concentration was observed. These concentration-dependent results are shown in *Fig. 4*. Moderate concentrations influence the line width and even change the sign of its temperature dependence. Such a concentration effect is due to intermolecular dipole-dipole interactions between the Gd^{3+} ions, as they become closer together in solution, and should be independent of magnetic field [21]. The effect is only noticeable at 2-mm-band, because the observed line widths are much smaller than at other frequencies. The curves in *Fig. 4* are the result of a least-squares fit with the line width represented by the sum of two *Arrhenius*-type functions, one proportional to the Gd^{3+} concentration.

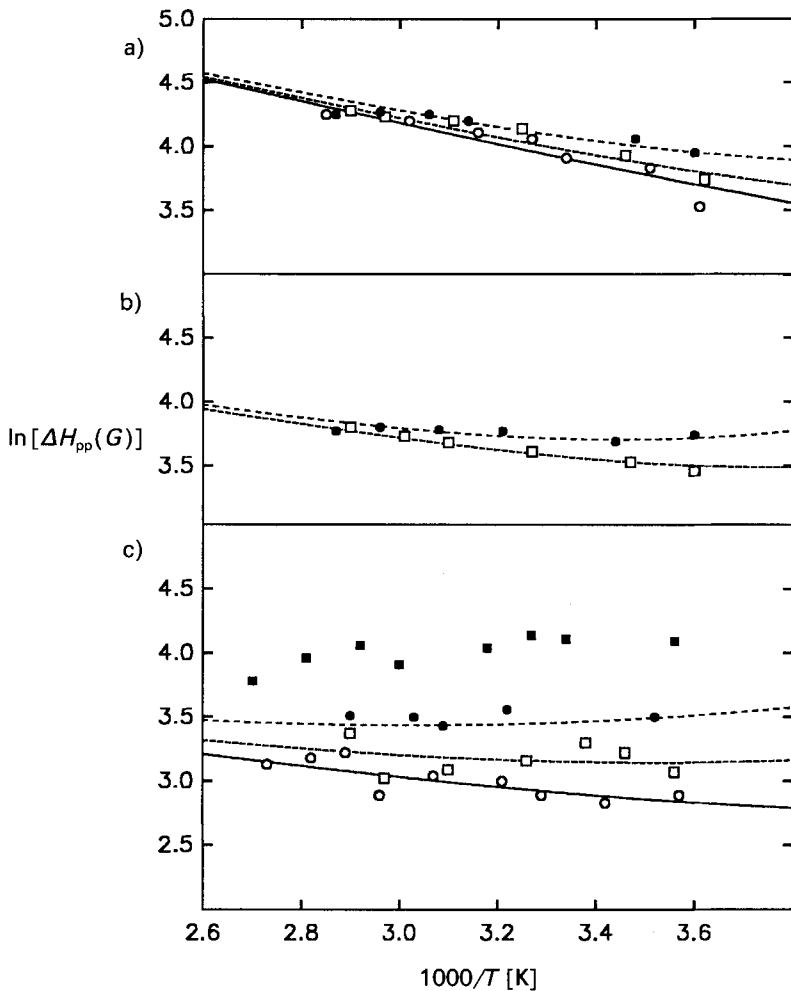


Fig. 4. Peak-to-peak EPR line widths measured at 2-mm-band (5.0 T) for a) 0.1m (●), 0.05m (□), and 0.02m (○) $[Gd(H_2O)_8]^{3+}$, b) 0.1m (●) and 0.05m (□) $[Gd(1)(H_2O)_2]^-$, and c) 0.35m (■), 0.11m (●), 0.05m (□), and 0.02m (○) $[Gd(2)(H_2O)]$

$$\Delta H_{pp} = A \exp \left\{ \frac{E_a}{R} - \left(\frac{1}{T} - \frac{1}{298.15} \right) \right\} + B [\text{Gd}^{3+}] \exp \left\{ \frac{E_b}{R} \left(\frac{1}{T} - \left(\frac{1}{298.15} \right) \right) \right\} \quad (20)$$

The fitted parameters were, for $[\text{Gd}(\text{H}_2\text{O})_8]^{3+}$: $A = 46.8 \pm 1.9 \text{ G}$, $E_a = -7.3 \pm 1.1 \text{ kJ mol}^{-1}$, $B = 116 \pm 34 \text{ G m}^{-1}$ and $E_b = 7.6 \pm 9.8 \text{ kJ mol}^{-1}$, for $[\text{Gd}(\mathbf{1})(\text{H}_2\text{O})_2]^-$: $A = 29.9 \pm 1.4 \text{ G}$, $E_a = -5.6 \pm 1.0 \text{ kJ mol}^{-1}$, $B = 109 \pm 19 \text{ G m}^{-1}$ and $E_b = 12.5 \pm 4.7 \text{ kJ mol}^{-1}$, and for $[\text{Gd}(\mathbf{2})(\text{H}_2\text{O})]$: $A = 14.4 \pm 1.1 \text{ G}$, $E_a = -5.0 \pm 1.7 \text{ kJ mol}^{-1}$, $B = 186 \pm 25 \text{ G m}^{-1}$ and $E_b = 6.4 \pm 3.8 \text{ kJ mol}^{-1}$. This approximation describes the data well in the range $0.02m$ to $0.11m$. One can, therefore, estimate the contribution of this intermolecular relaxation to the observed line widths. In the following analysis of the temperature and field dependence of the line widths, the results for the lowest concentrations are used in order to minimise this contribution. The line widths were corrected for the concentration-dependent contribution by subtracting the second term of Eqn. 20 with the fitted values of B and E_b . The concentrations are shown in Table 1 together with the magnitude of the correction.

Table 1. Concentrations of the Solutions Used for the EPR Line-Width Measurements Shown in Fig. 5. The magnitude of the correction made for the concentration-dependent contribution to the line width is given in brackets as a percentage of the total line width.

Frequency (magnetic field)	$[\text{Gd}(\text{H}_2\text{O})_8]^{3+}$	$[\text{Gd}(\mathbf{1})(\text{H}_2\text{O})_2]^-$	$[\text{Gd}(\mathbf{2})(\text{H}_2\text{O})]$
S-Band (0.14 T)	0.1m, pH 2.0 (2–4%)	No signal observable for 0.1m solution	0.35m, pH 3.95 (4–12%)
X-Band (0.34 T)	0.1m, pH 2.0 (2–6%)	0.1m, pH 5.0 (0.5–1%)	0.11m, pH 3.9 (2–5%)
K-Band (0.90 T) [22]	0.026m (1.0–1.1%)		
Q-Band (1.2 T)	0.1m, pH 2.0 (5–6%)	0.1m, pH 5.0 (1–10%)	0.11m, pH 3.9 (10–30%)
2-mm-Band (5.0 T)	0.02m, pH 2.0 (2–7%)	0.05m, pH 5.0 (6–28%)	0.02m, pH 3.9 (9–22%)

The variable-temperature, multiple-frequency, concentration-corrected line-width data for the three complexes are shown in Fig. 5. In the case of $[\text{Gd}(\text{H}_2\text{O})_8]^{3+}$, the corrected K-band data of *Marianelli* [22] are also shown. Several trends are noticeable.

i) At high temperatures and low fields, both the $[\text{Gd}(\text{H}_2\text{O})_8]^{3+}$ and $[\text{Gd}(\mathbf{1})(\text{H}_2\text{O})_2]^-$ data have a positive slope. For $[\text{Gd}(\text{H}_2\text{O})_8]^{3+}$, there is little dependence on magnetic field in this region.

ii) For $[\text{Gd}(\mathbf{2})(\text{H}_2\text{O})]$ and $[\text{Gd}(\mathbf{1})(\text{H}_2\text{O})_2]^-$ at low temperature and high fields, the slope is negative and, at a given temperature, the line width is approximately proportional to the inverse of the magnetic field.

iii) The $[\text{Gd}(\text{H}_2\text{O})_8]^{3+}$ and $[\text{Gd}(\mathbf{1})(\text{H}_2\text{O})_2]^-$ data exhibit a turnover between these two regions.

It is unlikely that the temperature dependence of τ_v can change sign. The dependence of line width on temperature in Fig. 1 must, therefore, display a maximum, if it is to be useful in describing the data. One can immediately conclude, therefore, that the represen-

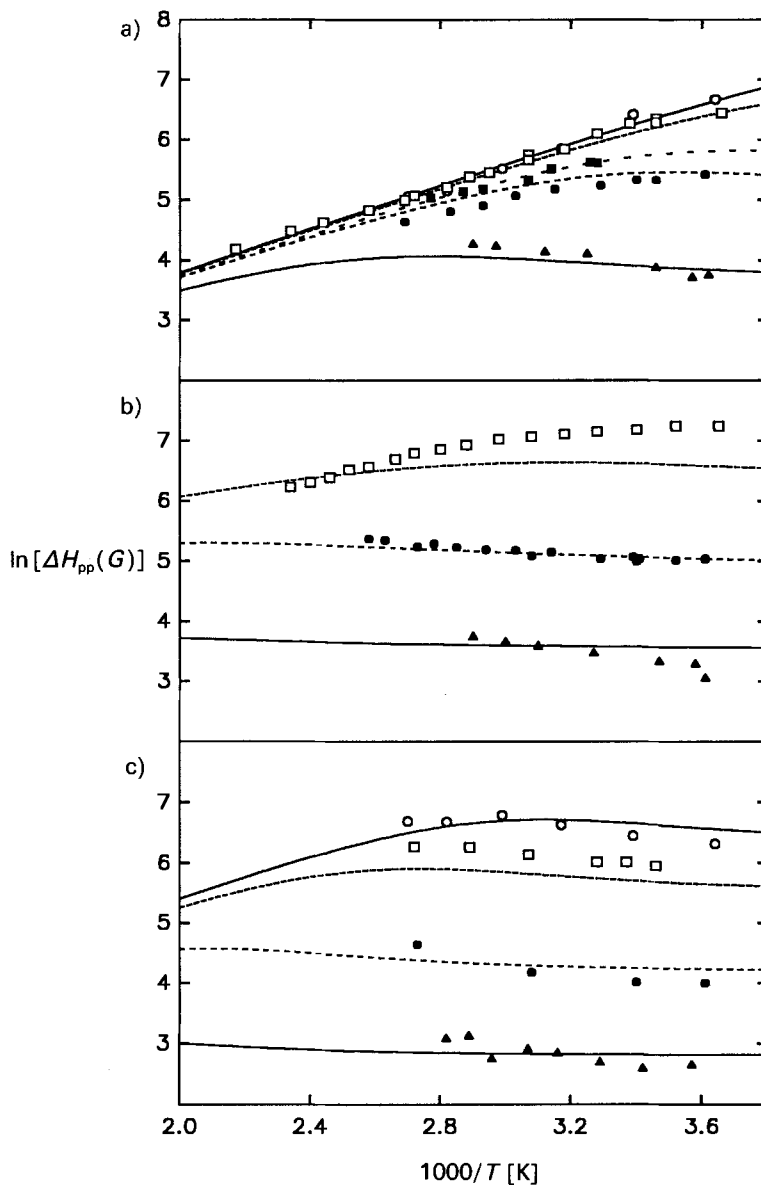


Fig. 5. Concentration-corrected peak-to-peak EPR line widths for a) $[Gd(H_2O)_8]^{3+}$, b) $[Gd(1)(H_2O)_2]^-$, and c) $[Gd(2)(H_2O)]$ measured at (○) S-band (0.14 T), (□) X-band (0.34 T), (■) K-band (0.9 T) [22], (●) Q-band (1.2 T), and (▲) 2-mm-band (5.0 T)

tation of the overall line width by the mean relaxation rate, $\langle 1/T_{2c} \rangle$, whether by *McLachlan's* theory as used by *Southwood-Jones et al.* [4] (Eqn. 5, Fig. 1b) or by calculation from the *Redfield* relaxation matrix is unrealistic. If one assumes, following *Reuben* [14], that the line width is determined by the narrowest transition (Eqn. 16, Fig. 1d), a turnover

from a positive slope at high temperatures and low fields to a negative slope at low temperatures and high fields is indeed predicted. However, at low temperatures and high fields, it is predicted that the line width is proportional to the inverse square of the magnetic field. We have been unable to fit the data for any of the complexes using *Eqns. 16 and 17*. If one associates the mean relaxation time, $\langle T_{2e} \rangle$, calculated from the *Redfield* relaxation matrix, with the line width (*Eqn. 19, Fig. 1f*), one also obtains the required turnover of slope. In addition, the line width at low temperatures and high fields is predicted to be approximately proportional to the inverse of the magnetic field, due to the second term in *Eqn. 19*.

We fitted the data, therefore, using *Eqn. 19* with *Eqn. 7* representing the temperature dependence of τ_v and $g = 2.0$ in *Eqn. 1*. The curves obtained from the least-squares fitting procedure are shown in *Fig. 5*, and the fitted parameters are listed in *Table 2*. To show that the influence of the correction for the concentration-dependent line widths is small, the parameters obtained from a fit of the uncorrected data are also listed. The parameters obtained by *Reuben* [14] are given for comparison.

Discussion. – Although the curves fitted to the data in *Fig. 5* are not perfect, they show that the EPR line widths of these Gd^{3+} complexes can be accounted for by modulation of the transient ZFS. The temperature and field dependence of the line widths can best be described using the mean relaxation time, $\langle T_{2e} \rangle$, calculated from the separate relaxation times obtained from the *Redfield* relaxation matrix, weighted by their intensities. Although this quantity had to be obtained numerically, the fitted *Eqn. 19* which describes the dependence of the overall line width on $\omega\tau_v$ is applicable to any Gd^{3+} complex in solution. One must, however, consider the region of validity of this equation. The first limitation is that the *Redfield* limit, $T_{1e}, T_{2e} > \tau_v$, must apply. The ‘worst case’ is $[\text{Gd}(\mathbf{2})(\text{H}_2\text{O})]$, for which, at room temperature, $\tau_v \approx 1.4 \times 10^{-10}$ s and $T_{2e} \approx 7 \times 10^{-11}$ s at S-band. For all other complexes and frequencies, the condition holds well. The second limitation is that *Eqn. 19* is only valid in the regime $\omega\tau_v \leq 10$. Using the fitted parameters given in *Table 2*, one can calculate the values of $\omega\tau_v^{298}$ for the three complexes at the different magnetic fields. These are, for $[\text{Gd}(\text{H}_2\text{O})_8]^{3+}$; 0.17 (S-band), 0.39 (X-band), 1.5 (Q-band), 5.9 (2-mm-band), for $[\text{Gd}(\mathbf{1})(\text{H}_2\text{O})_2]^-$; 2.9 (X), 11 (Q), and 44 (2-mm) and for $[\text{Gd}(\mathbf{2})(\text{H}_2\text{O})]$; 4.8 (S), 11 (X), 42 (Q), and 167 (2-mm). Thus, *Eqn. 19* is not strictly valid for $[\text{Gd}(\mathbf{1})(\text{H}_2\text{O})_2]^-$ at 2-mm-band and $[\text{Gd}(\mathbf{2})(\text{H}_2\text{O})]$ at S-, Q-, and 2-mm-bands. However, a fit of the data for these two complexes excluding the data for these fields results in only a small change of the fitted parameters (*Table 2*). One can, therefore, conclude that *a) Eqn. 19* is valid for $[\text{Gd}(\text{H}_2\text{O})_8]^{3+}$ at all measured frequencies, and describes the data very well. The parameters obtained from the least-squares fit must be physically meaningful. *b) Eqn. 19* describes reasonably well the data for the other two complexes, although it should be regarded as semi-empirical for $[\text{Gd}(\mathbf{1})(\text{H}_2\text{O})_2]^-$ at high magnetic fields and for $[\text{Gd}(\mathbf{2})(\text{H}_2\text{O})]$ at both high and low magnetic fields. The fitted parameters do not change significantly, when only the data for selected fields are fitted, so it seems that they must be meaningful. *c)* The fitted parameters allow extrapolation to different fields, but the limits of validity of *Eqn. 19* must be taken into account. One can also use the parameters to calculate the longitudinal relaxation times. As discussed in the theory section the longitudinal relaxation is very nearly single exponential for all $\omega\tau_v$, so that *Eqn. 4* due to *McLachlan* can be used within the *Redfield* limit.

Table 2. Parameters Obtained from the Least-Squares Fits of the EPR Line-Width Data

Complex in solution	Δ^2 [$\text{s}^{-2} \times 10^{20}$]	τ_v^{298} [s]	E_v [kJ mol^{-1}]
[Gd(H ₂ O) ₈] ³⁺	0.93 ± 0.04 1.00 ± 0.03 ^{a)} 1.1 ± 0.1 ^{b)}	(7.2 ± 0.7) × 10⁻¹² (6.7 ± 0.4) × 10 ^{-12a)} 5.04 × 10 ^{-12b)}	15.4 ± 1.1 15.0 ± 0.7 ^{a)} 11.0 ± 0.1 ^{b)}
[Gd(1)(H ₂ O) ₂] ⁻	0.80 ± 0.04 0.88 ± 0.03 ^{a)} 0.91 ± 0.04 ^{c)}	(4.8 ± 2.8) × 10⁻¹¹ (5.0 ± 2.0) × 10 ^{-11a)} (5.9 ± 2.6) × 10 ^{-11c)}	10.2 ± 6.3 12.0 ± 4.2 ^{a)} 13.7 ± 4.8 ^{c)}
[Gd(2)(H ₂ O)]	0.38 ± 0.02 0.46 ± 0.01 ^{a)} 0.57 ± 0.01 ^{d)}	(1.4 ± 1.0) × 10⁻¹⁰ (1.9 ± 1.0) × 10 ^{-10a)} (2.7 ± 0.9) × 10 ^{-10d)}	17.6 ± 10.0 23.0 ± 8.0 ^{a)} 29.0 ± 4.0 ^{d)}
[Gd(cacodylate)]	1.4 ± 0.1 ^{b)}	6.7 × 10 ^{-12b)}	15.3 ± 0.7 ^{b)}
[Gd(BSA)]	0.615 ± 0.015 ^{b)}	7.65 × 10 ^{-12b)}	7.1 ± 0.9 ^{b)}

^{a)} Obtained from a fit of the data uncorrected for the concentration-dependent line width.

^{b)} Parameters obtained by *Reuben* [14].

^{c)} Obtained from a fit of X- and Q-band data only.

^{d)} Obtained from a fit of X-band data only.

The values that we obtained for τ_v^{298} , E_v , and Δ^2 are compared in *Table 2* with those obtained by *Reuben* [14] from X- and Q-band EPR measurements on a series of Gd³⁺ complexes in aqueous solution. The results we obtain for the aqua ion are very similar to those obtained by *Reuben*. This is not surprising, since the approach used by *Reuben* (see theory section) is valid in this case for the two fields he measured (no turnover of the slope). We consider that our values are better defined, because of the wider range of temperature and magnetic field probed. Because the correlation time, τ_v , has been found to be shorter than estimates for the rotational correlation time of complexes in solution, it has been associated with transient distortions of the complex, which produce a transient ZFS [10] [13] [14]. To explain EPR line shapes in aqueous Mn²⁺ solutions, an alternative picture has been presented, where the distortions of the aqua complex are long lived ($> 10^{-9}$ s) and τ_v is determined by the rotation of the complex, which is very rapid ($\tau_c^{298} \approx 10^{-12}$ s) due to the high degree of disordering between the two differently ordered regions (complex and bulk) [23]. In the case of the Gd³⁺ aqua complex, we find that the room-temperature correlation time, $\tau_v^{298} = (7.2 \pm 0.7) \times 10^{-12}$ s, is much shorter than expected for the rotational correlation time of the complex ($\tau_c^{298} \approx 2.5 \times 10^{-11}$ s from ¹⁷O-NMR measurements [2]), so we are drawn to the conclusion that the former picture is the more realistic. For the complexes with **1** and **2**, the correlation times, $\tau_v^{298} = (4.8 \pm 2.8) \times 10^{-11}$ s and $\tau_v^{298} = (1.4 \pm 1.0) \times 10^{-10}$ s, are much longer and approach the order of magnitude expected for rotation of the complexes ($\tau_c^{298} \approx 7 \times 10^{-11}$ s and $\tau_c^{298} \approx 1.6 \times 10^{-10}$ s for the **1** and **2** complexes, respectively [2] [6]). This may be due to the complexes with the large ligands being more rigid than the aqua complex. Such an effect would be consistent with the reduced values of Δ^2 observed as the correlation time increases, since the increased rigidity would presumably also reduce the magnitude of the transient ZFS. It is surprising that a similar trend was not observed by *Reuben* [14] (*Table 2*) for the complexes with the dimethyl arsinato (cacodylate) and bovine serum albumin (BSA) molecules. However, the theoretical approach he used (see theory section) was not strictly valid, according to our work. This is only evident now because of the

larger number of magnetic fields and larger temperature range at which we were able to make measurements.

Using *Eqns. 4 and 19* with the parameters in *Table 2*, one can calculate the expected magnetic-field dependence of the longitudinal and mean transverse electronic relaxation times for the three complexes (*Fig. 6*), and estimate the effect of electronic relaxation on their proton relaxivities. The inner-sphere proton relaxivity may be described by the *Solomon-Bloembergen* equations and modifications thereof [24]. The longitudinal relaxation is normally governed by the dipolar contribution which may be written as

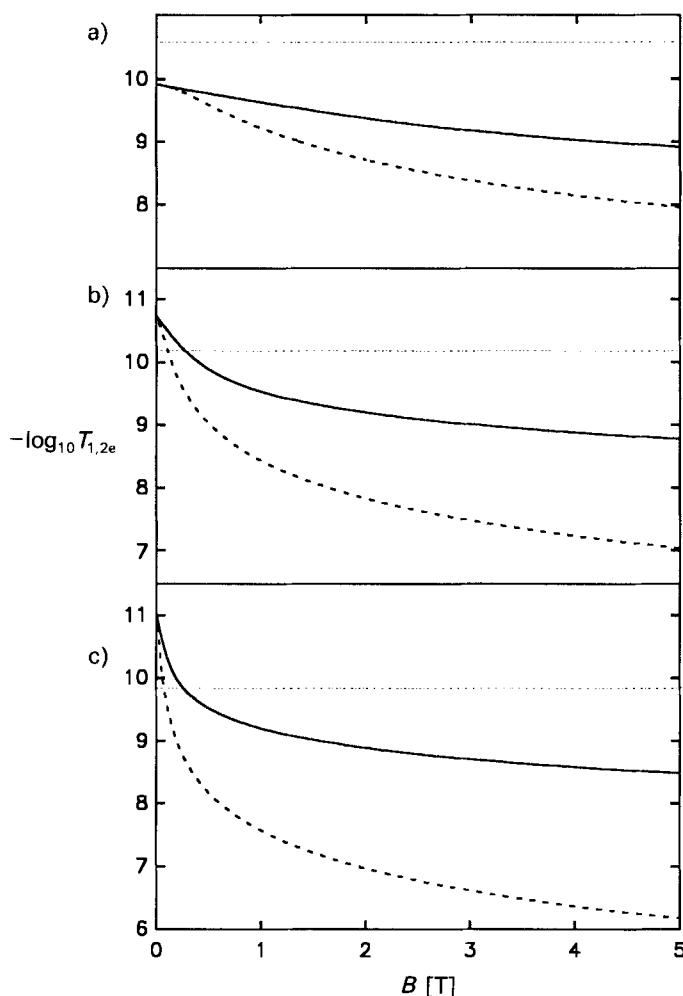


Fig. 6. Predicted magnetic-field dependence of the longitudinal (dashed line) and transverse (solid line) electronic relaxation rates of Gd^{3+} in solutions of a) $[Gd(H_2O)_8]^{3+}$, b) $[Gd(\mathbf{1})(H_2O)_2]^-$, and c) $[Gd(\mathbf{2})(H_2O)]$ at 298.15 K. The horizontal dot-dashed lines indicate the values of τ_c estimated from ^{17}O -NMR results [2] [6].

$$\frac{1}{T_{1e}} = K \left[3 \frac{\tau_{c1}}{1 + (\omega_1 \tau_{c2})^2} + 7 \frac{\tau_{c2}}{1 + (\omega \tau_{c2})^2} \right] \quad (21)$$

where

$$\tau_{c1}^{-1} = \tau_c^{-1} + \tau_m^{-1} + T_{1e}^{-1}$$

$$\tau_{c2}^{-1} = \tau_c^{-1} + \tau_m^{-1} + T_{2e}^{-1}$$

K is a constant, τ_c is the rotational correlation time of the complex, τ_m is the binding time of a water proton in the inner sphere, ω_1 is the proton-resonance frequency, and ω is the electron-resonance frequency. We postpone a full discussion until our ^{17}O -NMR results are finalised [2] [6], but, estimating that $10^{-9} < \tau_m < 10^{-5}$ s and using the values for τ_c^{298} mentioned above, one can see from *Fig. 6* that, for $[\text{Gd}(\mathbf{1})(\text{H}_2\text{O})_2]^-$ and $[\text{Gd}(\mathbf{2})(\text{H}_2\text{O})]$, the electronic relaxation will become the dominant correlation time at sufficiently low magnetic fields. The outer-sphere proton relaxivity depends on a correlation time describing the diffusion of the H_2O molecules away from the complex, and the electronic relaxation times [1]. To describe correctly the field-dependent proton relaxivity (NMRD profiles) for these complexes, it will be necessary to take account of the field dependence of the electronic relaxation and of the difference between longitudinal and transverse electronic relaxation times.

Conclusions. – The magnetic-field-dependent line width of the complexes $[\text{Gd}(\text{H}_2\text{O})_8]^{3+}$, $[\text{Gd}(\mathbf{1})(\text{H}_2\text{O})_2]^-$, and $[\text{Gd}(\mathbf{2})(\text{H}_2\text{O})]$ in aqueous solution can be explained by the modulation of the ZFS, where the overall line width is described by the intensity-weighted mean transverse relaxation time obtained from diagonalisation of the appropriate *Redfield* relaxation matrix. Fits of the data yield a correlation time for this modulation which, in the case of the aqua complex, is too short to be due to rotational motion, and so is ascribed to transient distortions of the complex. For $[\text{Gd}(\mathbf{1})(\text{H}_2\text{O})_2]^-$ and $[\text{Gd}(\mathbf{2})(\text{H}_2\text{O})]$, the correlation time is long compared to that for the aqua complex, consistent with the complexes with the large ligands being more rigid.

This work provides an experimental and theoretical basis for the understanding of the contribution of electronic relaxation to the proton relaxivity of these complexes as determined by NMR dispersion measurements. Care should be taken, however, with the extent of validity of the theoretical approach.

We wish to thank Mr. *S. Chemerisov* for his help with the 2-mm-band measurements and *Nycomed Salutar Inc.* and *Sterling Winthrop* for their financial and scientific contributions. One of us (*G.G.*) thanks the *SCIENCE* program of the *European Community* for the provision of a research fellowship. This work was supported by the *Swiss National Science Foundation*.

REFERENCES

- [1] S. H. Koenig, R. D. Brown III, *Progress NMR Spectrosc.* **1990**, *22*, 487.
- [2] K. Micskei, D. H. Powell, L. Helm, E. Brücher, A. E. Merbach, *Magn. Reson. Chem.*, in press.
- [3] C. F. G. C. Geraldès, R. D. Brown III, E. Brücher, S. H. Koenig, A. D. Sherry, M. Spiller, *Magn. Res. Med.* **1992**, *27*, 284.
- [4] R. V. Southwood-Jones, W. L. Earl, K. E. Newman, A. E. Merbach, *J. Chem. Phys.* **1980**, *73*, 5909.
- [5] A. D. McLachlan, *Proc. R. Soc. London [Ser.] A* **1964**, *280*, 271.

- [6] G. Gonzalez, D. H. Powell, V. Tissières, A. E. Merbach, submitted for publication.
- [7] L. Helm, A. E. Merbach, *Eur. J. Solid State Inorg. Chem.* **1991**, 28, 245.
- [8] M. Furrer, Doctoral Thesis No. 5339, ETH-Zürich 1974.
- [9] L. Ehnbom, B. F. Pedersen, *Acta Chim. Scand.* **1992**, 46, 126.
- [10] N. Bloembergen, L. O. Morgan, *J. Chem. Phys.* **1961**, 34, 842.
- [11] A. Hudson, G. R. Luckhurst, *Mol. Phys.* **1969**, 16, 395.
- [12] B. R. McGarvey, *J. Phys. Chem.* **1957**, 61, 1232.
- [13] M. Rubinstein, A. Baram, Z. Luz, *Mol. Phys.* **1971**, 20, 67.
- [14] J. Reuben, *J. Phys. Chem.* **1971**, 75, 3164.
- [15] A. Hudson, J. W. E. Lewis, *Trans. Faraday Soc.* **1970**, 66, 1297.
- [16] A. Abragam, 'The Principles of Nuclear Magnetism', Oxford University, London, 1961.
- [17] A. K. Gregson, D. M. Dodderell, D. T. Pegg, *Aust. J. Chem.* **1978**, 31, 469.
- [18] E. U. Condon, G. H. Shortley, 'The Theory of Atomic Spectra', Cambridge University Press, 1959.
- [19] H. L. Friedman, M. Holz, H. G. Hertz, *J. Chem. Phys.* **1978**, 70, 3369.
- [20] Ya. S. Lebedev, in 'Modern Pulsed and Continuous Wave Electron Spin Resonance', Eds. L. Kevan and M. Bowman, Wiley, New York, 1990.
- [21] C. C. Hinckley, L. O. Morgan, *J. Chem. Phys.* **1966**, 44, 989.
- [22] R. Marianelli, Ph. D. Thesis, University of California, Lawrence Radiation Lab. Report UCRL-17069, 1966.
- [23] L. Burlamacchi, G. Martini, M. F. Ottaviani, M. Romanelli, *Adv. Molec. Relaxation Interaction Processes* **1978**, 12, 145.
- [24] J. Kowalewski, L. Nordensköld, N. Benetis, P.-O. Westlund, *Progress NMR Spectrosc.* **1985**, 17, 141.